Development 137, 3615-3624 (2010) doi:10.1242/dev.056408

Embryonic multipotent progenitors remodel the *Drosophila* airways during metamorphosis

Chrysoula Pitsouli[1,*] and Norbert Perrimon[1,2,*]

SUMMARY

Adult structures in holometabolous insects such as *Drosophila* are generated by groups of imaginal cells dedicated to the formation of different organs. Imaginal cells are specified in the embryo and remain quiescent until the larval stages, when they proliferate and differentiate to form organs. The *Drosophila* tracheal system is extensively remodeled during metamorphosis by a small number of airway progenitors. Among these, the spiracular branch tracheoblasts are responsible for the generation of the pupal and adult abdominal airways. To understand the coordination of proliferation and differentiation during organogenesis of tubular organs, we analyzed the remodeling of *Drosophila* airways during metamorphosis. We show that the embryonic spiracular branch tracheoblasts are multipotent cells that express the homeobox transcription factor Cut, which is necessary for their survival and normal development. They give rise to three distinct cell populations at the end of larval development, which generate the adult tracheal tubes, the spiracle and the epidermis surrounding the spiracle. Our study establishes the series of events that lead to the formation of an adult tubular structure in *Drosophila*.

KEY WORDS: Cut, *Drosophila*, Spiracular branch, Tracheoblasts

INTRODUCTION

Many organs in the human body, such as the lung, kidney and mammary gland, develop in the embryo from simple epithelial sheets that fold, branch and ramify into complex tubular structures. Tubular organs arise from embryonic progenitors that proliferate and differentiate to generate the different cell types that constitute the final functional organ. Their morphogenesis is dynamic and is based on cell division, growth, cell shape changes and migration, as well as on cell death. The spatiotemporal coordination of these processes governs normal development, while errors lead to diseases such as lung agenesis and polycystic kidney disease (Lu et al., 2006). Moreover, tube-containing organs, such as the lung and mammary gland, harbor epithelial stem cells that become activated after environmental assaults or hormonal stimulation (LaBarge et al., 2007; Rawlins and Hogan, 2006). Importantly, regeneration and repair often recapitulate normal developmental events (Rawlins, 2008). Therefore, characterization of the mechanisms operating during organogenesis is important for understanding not only development and disease pathogenesis but also regeneration. Studies at the cellular and molecular levels in *C. elegans* and *Drosophila* have revealed many commonalities in tubular organ development, despite the immense variability in their shapes and functions (Hogan and Kolodziej, 2002; Lu et al., 2006).

Drosophila has provided a wealth of information regarding the early specification of the embryonic airway precursors, as well as the molecular events involved in tubulogenesis and branching morphogenesis (Ghabrial et al., 2003; Manning and Krasnow, 1993). The embryonic trachea develops from 10 bilaterally symmetric clusters (Tr1-Tr10) of ~80 cells that express the transcription factor Trachealess (Trh). These cells invaginate to form epithelial sacs that remain connected to the epidermis through a small stalk, the spiracular branch (SB) (Ghabrial et al., 2003; Manning and Krasnow, 1993). They then differentiate under the control of FGF/Branchless (Bnl), spread and generate a network of ~10,000 interconnected tubes. Critical signaling molecules involved in tube formation and branching morphogenesis, such as FGF/Bnl (Sutherland et al., 1996) and Sprouty (Spry), a negative regulator of RTK (Hacohen et al., 1998), were first identified in the embryonic *Drosophila* trachea, and were later shown to play strikingly similar roles in mammalian tubular organogenesis. For example, FGF10, the mammalian homologue of Bnl, which signals through FGFR2, was shown to drive lung development (Min et al., 1998) and to play a key role in lung regeneration following injury (Warburton et al., 2001), while Spry2 was found to negatively regulate tube formation in mice by inhibiting FGFR signaling (Tefft et al., 1999). In addition, NPAS3, a mammalian homologue of the *Drosophila* transcription factor Trh, has been shown to play a role in lung development and homeostasis (Zhou et al., 2009).

Although studies of the *Drosophila* embryonic trachea have increased our understanding of tube formation and branching morphogenesis, the events that take place during development of branched organs, such as the lung and the kidney, where cell proliferation and differentiation have to be coordinated, cannot be extensively modeled in the fly embryo because morphogenesis of the embryonic trachea proceeds without cell division. The remodeling of the *Drosophila* tracheal system at the larval/pupal stages, however, provides an opportunity to analyze the coordination of proliferation and differentiation during morphogenesis of the tracheoblasts, which are the airway progenitors of the adult tracheal system.

The adult tracheal system of *Drosophila* is composed mainly of the spiracles, the external respiratory organs, and the gas-transporting tracheal tubes to which they are connected. Each spiracle opens to the epidermis and is surrounded by epidermal cells, the perispiracular epidermis that arises from the spiracular

[1]Department of Genetics, Harvard Medical School, 77 Avenue Louis Pasteur, Boston, MA 02115, USA. [2]Howard Hughes Medical Institute, Harvard Medical School, 77 Avenue Louis Pasteur, Boston, MA 02115, USA.

*Authors for correspondence (cpitsouli@receptor.med.harvard.edu; perrimon@receptor.med.harvard.edu)

Accepted 24 August 2010

nest of the abdominal histoblasts during morphogenesis of the abdominal epidermis in the pupae (Ninov et al., 2007; Roseland and Schneiderman, 1979). The tracheal tubes originate from imaginal precursors, the tracheoblasts, that are set aside in the embryo and remain quiescent until the third larval instar when they rapidly proliferate and differentiate to form new tubes during metamorphosis (Whitten, 1980). Different tracheoblast populations can be distinguished based on their locations and the different parts of the pupal and adult tracheal system they generate. These include the imaginal tracheoblast populations located on the SBs (Manning and Krasnow, 1993; Samakovlis et al., 1996a; Weaver and Krasnow, 2008; Whitten, 1980) (also see Results), the air sac primordium (ASP), and the Tr2 and the dorsal branch (DB) tracheoblasts (Cabernard and Affolter, 2005; Guha and Kornberg, 2005; Guha et al., 2008; Sato et al., 2008; Sato and Kornberg, 2002; Weaver and Krasnow, 2008).

In this work, we focus on the abdominal SB tracheoblasts and describe how these progenitors proliferate and differentiate to generate diverse cell types that form a functional trachea. We demonstrate that the embryonic SB tracheoblasts are multipotent cells, express the transcription factor Cut that is necessary for the survival and normal development of the abdominal airways, and contribute to different parts of the adult tracheal system. Contrary to prior beliefs (Manning and Krasnow, 1993; Robertson, 1936; Roseland and Schneiderman, 1979; Whitten, 1980), we demonstrate that SB cells generate the spiracle and its surrounding epidermis as well as the adult tracheal tubes. Altogether, our study establishes the series of cellular events that coordinate formation of an adult tubular structure in *Drosophila*.

MATERIALS AND METHODS

Fly stocks

Descriptions of the following stocks, unless indicated, can be found in FlyBase. Numbers in parentheses correspond to Bloomington stock numbers: *btl-Gal4 UAS-actGFP* (#8807), *UAS-srcGFP* (#5432), *fzr-lacZ^{G0326}* (#12241), *tub-Gal80^{ts}* (#7016) (McGuire et al., 2004), *cut-Gal4* (PG142) (Bourbon et al., 2002), *UAS-cut* (gift from B. Mathey-Prevot), *UAS-cut^{RNAi}* (VDRC#5687) (Dietzl et al., 2007), *esg-Gal4 tub-Gal80^{ts} UAS-EGFP* (Micchelli and Perrimon, 2006), *UAS-FLP* (Duffy et al., 1998), *act5C-FRT-stop-FRT-lacZ* (Struhl and Basler, 1993) and *hsFLP; act5C-FRT-stop-FRT-Gal4 UAS-GFP* (Ito et al., 1997).

Generation of mitotic clones

For wild-type MARCM clones, *hsFLP tub-Gal4 UAS-nlsGFP; tub-Gal80 FRT40A/UbiGFP FRT40A* or *hsFLP tub-Gal4 UAS-nlsGFP; FRT82B tub-Gal80/FRT82B arm-lacZ* (Lee and Luo, 2001) were used. In addition, wild-type FLPout clones were generated using *hsFLP; act5C-FRT-stop-FRT-Gal4 UAS-GFP* flies (Ito et al., 1997).

To assess *cut* mutant mosaics, we used *cut^{DB7} FRT18D/Ubi-Histone-GFP FRT18D; hsFLP* (Sun and Deng, 2005) larvae. Clones ectopically expressing *cut* were induced in *hsFLP; act5C-FRT-stop-FRT-Gal4 UAS-GFP/UAS-cut* larvae.

Lineage tracing

A *UAS-FLP*; *act5C-FRT-stop-FRT-lacZ* stock was crossed to *btl-Gal4 UAS-srcGFP* and *cut-Gal4; UAS-srcGFP* in the absence or presence of a *tub-Gal80^{ts}* transgene to allow temporal activation of the Gal4 and hence the FLPase. To induce early lineage clones, crosses were constantly kept at 25°C, while, for late clones, crosses were kept at 18°C until the L2 stage and then transferred to 29°C to inactivate the Gal80 repressor.

Screen

We screened a collection of monoclonal antibodies targeting *Drosophila* proteins obtained from the Development Studies Hybridoma Bank (DSHB). All monoclonal supernatants were used at 1:20 dilution for screening. Different Gal4 drivers with documented expression in the tracheal system were pre-selected from the *Drosophila* Genetics Resource Center (DGRC) and were screened for expression in the larval tracheal system by crossing to *UAS-EGFP* and analyzing L3 larvae.

Immunohistochemistry

For all experiments, phenotypes are assessed at the wandering third instar stage (110-120 hours AEL), except in Fig. 2 where a complete developmental series of the SB is shown. Third instar wandering larvae were ventrally filleted in dissection chambers (Budnik et al., 2006), ensuring that the tracheal system remained intact and the SBs were not broken off from the epidermis. After removal of the internal organs, the larval carcass with the associated trachea was fixed for 20 minutes at room temperature with 4% formaldehyde/PBS and treated as described (Pitsouli and Delidakis, 2005). Younger larvae were glued onto sylgard-coated coverslips, ventrally filleted and fixed as above. Embryos were stained using standard procedures.

The following antibodies were used: mouse-anti-Cut 2B10, mouse-anti-Hnt 1G9, mouse-anti-Cyclin A, mouse-anti-Cyclin B and rat-anti-DCAT2 (1:50-1:100, DSHB), rabbit-anti-β-gal (1:10,000, Cappel), mouse-anti-β-gal (1:500, Promega), rabbit-anti-phospho-histone H3 (1:3000, Millipore) and rabbit-anti-GFP (1:2000, Molecular Probes). Anti-mouse or anti-rabbit secondary antibodies conjugated to Alexa-Fluor 488, 555, 594 and 647 were used at 1:1000. To stain nuclei, DAPI was used at 0.3 μg/ml along with the secondary antibodies.

Fluorescent images were acquired with a Leica TCS SP2 AOBS or a TCS DM-IRE2 AOBS confocal microscope. Time-lapse imaging of *btl-Gal4 UAS-actGFP* pupae was performed by placing the pupa in a drop of halocarbon oil 700 in a chamber slide followed by imaging with a TCS DM-IRE2 AOBS confocal inverted microscope.

Adult phenotypes and X-gal staining

LacZ-expressing flies were dissected in 1×PBS and fixed in 4% formaldehyde/PBS for 30 minutes at room temperature. After removal of the fixative, the tissues were incubated in X-gal colorization solution for several hours at 37°C. Dissected abdomens were mounted in Hoyer's and incubated overnight at 65°C. Transmitted light images were acquired using a Zeiss Axiophot equipped with a CCD camera.

EdU labeling

The Click-iT EdU Alexa-Fluor 594 (Molecular Probes, Invitrogen) was used to detect cells in S-phase following the manufacturer's protocol. In short, ventrally filleted *btl-Gal4 UAS-srcGFP* larvae were incubated in 100 μM EdU in 1×PBS for 1 hour at 25°C in a humid chamber to allow incorporation of the analogue into the DNA of replicating cells. Subsequently, the tissue was fixed for 20 minutes in 4% formaldehyde/PBS at room temperature. Following two brief washes with 3% BSA in PBS and permeabilization for 20 minutes with 0.5% Triton-X in PBS, EdU was visualized using fresh Click-iT reaction cocktail. After incubation for 30 minutes and three washes in 3% BSA, 0.5% Triton-X in PBS, samples were co-stained with DAPI to visualize nuclei and mounted in Vectashield (Vector Laboratories).

DNA content

Confocal sections (0.1 μm) of DAPI-stained nuclei with unsaturated signal were used to generate additive projections with ImageJ. Total DAPI fluorescence intensity per nucleus was measured as mean pixel intensity × number of pixels per nucleus. DAPI intensities of more than 40 cells were measured in Zone 1 and Zone 3 of single SB clusters.

RESULTS

Morphogenesis of the SB tracheoblasts from the embryo to adult

To analyze how proliferation and differentiation are coordinated during tracheoblast development, we studied the morphogenesis of the abdominal Tr4 and Tr5 SBs (Fig. 1A-C,G) as they are easily visualized following ventral filleting of the larvae and give rise to specialized pupal tracheoles used for oxygenation of the posterior of the animal during metamorphosis (Weaver and Krasnow, 2008;

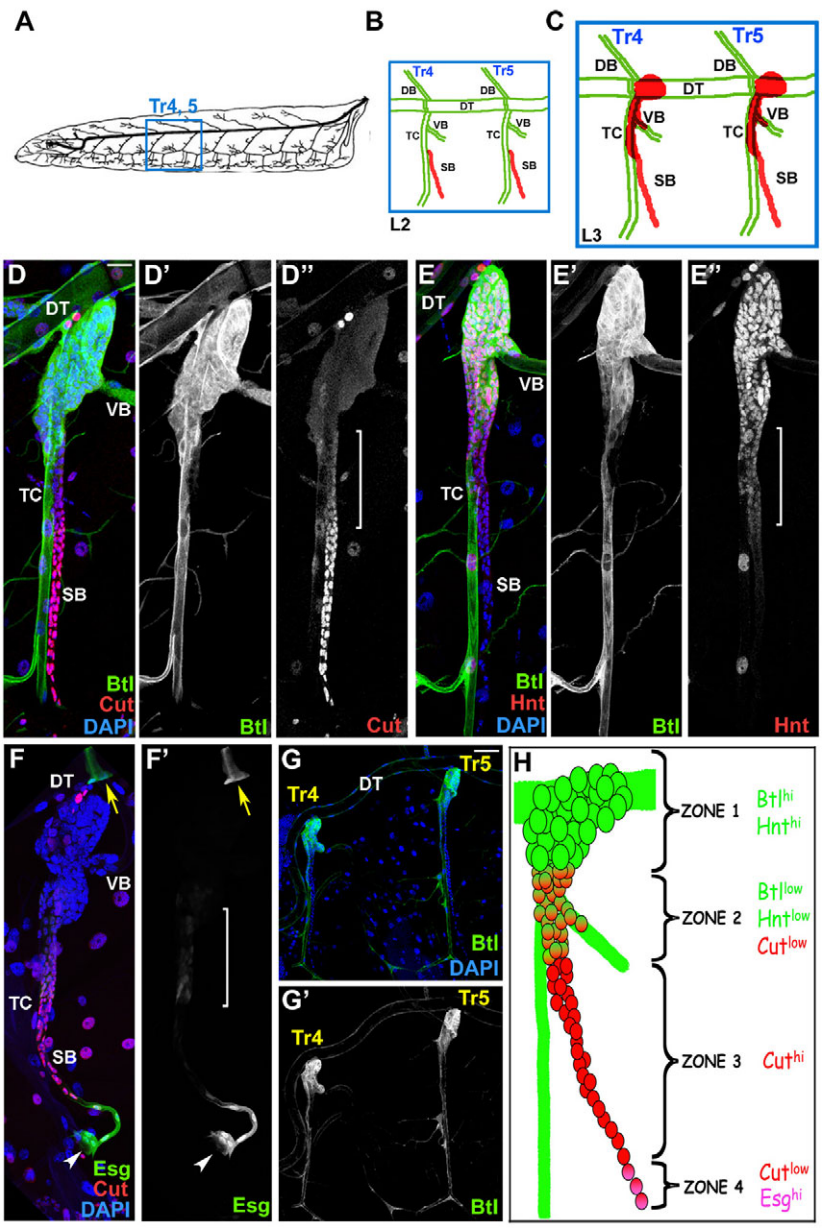

Fig. 1. The transcription factors Cut, Hindsight and Escargot, and FGFR/Breathless, label the SB tracheoblasts in the late *Drosophila* larva. (**A**) Schematic of a *Drosophila* third instar larval tracheal system; blue box demarcates Tr4 and Tr5. (**B**) Schematic of the boxed region in A of an early larva (L1-L2), indicating the different tracheal branches (DB, dorsal branch; DT, dorsal trunk; TC, transverse connective; VB, visceral branch; SB, spiracular branch). The SB (red) corresponds to the original location of the SB tracheoblasts, whereas all other branches (green) correspond to gas-transporting Btl-positive tubes. (**C**) Schematic of the boxed region in A of a late L3 larva/early pupa; the SB cells (red) have proliferated and migrated on the TC, VB and DT. (**D-D″**) *btl-Gal4 UAS-GFP* (green in D,D′) L3 larva stained for Cut (red in D,D″) and DAPI (blue); Cut is also present in differentiated muscle cells with large nuclei. (**E-E″**) *btl-Gal4 UAS-GFP* (green in E,E′) L3 larva stained for Hnt (red in E,E″) and DAPI (blue); Hnt is expressed in all gas-transporting tracheal cells. (**F**,**F′**) *esg-Gal4 UAS-GFP* (green) late L3 larva stained for Cut (red) and DAPI (blue). White arrowheads show Esg+ Zone 4 cells and yellow arrows mark the Esg+ fusion cell on the DT. Cut is not expressed in the fusion cell. Brackets in D″,E″,F′ indicate Zone 2. (**G**,**G′**) Low-magnification view of the Tr4 and Tr5 of a *btl-Gal4 UAS-GFP* (green) L3 larva labeled with DAPI (blue). Scale bar: 20 μm in A-F′; 40 μm in G,G′. (**H**) Schematic of the four different Zones of the SB.

Whitten, 1980). SB cells are epithelial in origin and express E-cadherin (see Fig. S1A-C in the supplementary material). They are set aside in each embryonic tracheal metamere (Tr1-Tr10), and, unlike gas-transporting cells, do not express FGFR/Breathless (Btl) (Samakovlis et al., 1996a), as shown in *btl-Gal4 UAS-actGFP* animals (Fig. 1B,C,G; Fig. 2D).

Tr4 and Tr5 SB cells form a stalk that connects to the epidermis and remain quiescent until the third larval instar (L3) when they start proliferating (Fig. 1A-C; Fig. 2D-J). SB tracheoblasts migrate progressively on the transverse connective (TC), the visceral branch (VB) and the dorsal trunk (DT) (Fig. 1B-C; see Fig. S1D in the supplementary material), eventually remodeling the pupal and adult tracheal systems (Weaver and Krasnow, 2008; Whitten, 1980).

SB tracheoblasts represent a heterogeneous cell population with distinct mitotic properties

To identify genes expressed in the SB tracheoblasts, we screened a collection of monoclonal antibodies and a number of Gal4-expressing lines (see Materials and methods). We found that the developing tracheoblast population in late L3 larvae could be subdivided into four zones (Fig. 1H) based on the expression patterns of four proteins: FGFR/Btl, which is always expressed in differentiated tracheal cells (Manning and Krasnow, 1993; Samakovlis et al., 1996a); Hindsight (Hnt), a Ras Responsive Element Binding Protein-1 (RREBP-1) homologue that has been shown to have a structural role in tracheal tubes (Wilk et al., 2000); Cut, a homeobox transcription factor with very broad tissue expression in flies and mammals (Nepveu, 2001; Sansregret and Nepveu, 2008); and Escargot (Esg), a transcriptional repressor necessary for tube fusion in the trachea and for maintaining diploidy of imaginal cells (Fuse et al., 1994; Hayashi et al., 1993; Samakovlis et al., 1996b). Zone 1 is distinguished by high levels of both Btl and Hnt, and encompasses large cells associated with the TC, DT and VB. Zone 2 cells express Btl, Hnt, Cut, as well as Esg at low levels. Cells in Zone 3 express high levels of Cut and exhibit spindle-like nuclei. Cells in this zone constitute the SB tube that connects to the epidermis. Finally, cells in Zone 4 express low levels of Cut and high levels of Esg, and constitute the spiracular

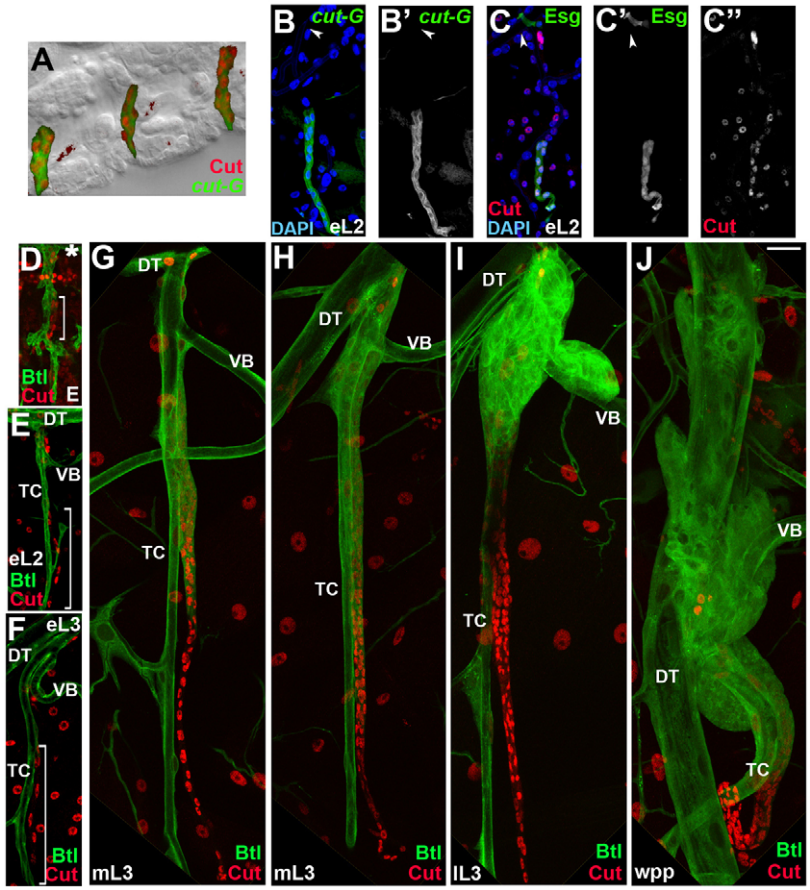

Fig. 2. The SB tracheoblast clusters grow extensively during the L3 stage. (**A**) SB tracheoblasts of a stage 15 *cut-Gal4; UAS-srcGFP* (green) *Drosophila* embryo stained for Cut (red); three tracheal segments are shown overlaid on a phase-contrast image of the embryo. Membrane-tagged srcGFP highlights the close association of the SB with the embryonic epidermis. (**B**,**B′**) Early L2 (48 hours AEL) *cut-Gal4; UAS-srcGFP* (green) larva stained for DAPI (blue); all SB cells are Cut+. (**C-C″**) Early L2 (48 hours AEL) *esg-Gal4 UAS-EGFP* (green in C,C′) larva stained for Cut (red in C,C″) and DAPI (blue); all SB cells co-express Cut and Esg (outside the SB, Cut stains muscle nuclei). Arrowheads in B and C indicate the DT. (**D-J**) Development of the Tr5 SB tracheoblast cluster in *btl-Gal4 UAS-GFP* (green) animals stained for Cut (red). (D) Stage 15 embryo. (E) Early L2 larva (48 hours AEL). (F) Early L3 larva (72 hours AEL). (G) Mid-L3 larva (90 hours AEL). (H) Mid-L3 larva (100 hours AEL). (I) Wandering late L3 larva (120 hours AEL). (J) White prepupa (121 hours AEL). Brackets in D-F indicate the SB Cut+ cells. Scale bar: 20 μm.

nest of the abdominal histoblasts (Fig. 1D-F). Interestingly, Btl and Hnt always label the same cells and their expression is complementary to Cut expression. The inverse graded expression of Btl/Hnt and Cut along the SB cluster, which generates a zone where all markers (including Esg) are expressed at low levels (Fig. 1D″,E″,F′,H), suggests that Zone 2 might be a fate transition zone for both Zones 1 and 3.

To understand the origin of the abdominal SB tracheoblasts present at late L3, we examined the expression of Btl, Hnt, Cut and Esg at earlier developmental stages. At embryonic stage 15 (Fig. 2A), each SB tracheoblast cluster consists of 8-11 Cut-positive/Esg-positive cells that do not express Btl (Fig. 2D). Subsequently, during L2 to early L3, SB cells elongate to follow body growth (Fig. 2B-F), and after an active proliferation phase during L3, they reach about 250-300 cells in each Tr4 and Tr5 cluster (Fig. 2G-J). FGFR/Btl (visualized by *btl-Gal4 UAS-GFP*) and Hnt expression starts at the early L3 stage in these clusters at the SB/TC junction that will form Zone 2 (Fig. 2F,G). Interestingly, during larval development the relative location of Cut-positive and Hnt/Btl-positive cells does not change (Fig. 2), so that they always constitute adjacent populations overlapping at the TC/SB junction. By contrast, Esg shows a more dynamic expression pattern, but is always strongly expressed in the spiracular histoblasts (Zone 4) close to the epidermis (Fig. 1F).

To understand the proliferative properties and characterize the differentiation state of the SB cells, we conducted a cell cycle analysis at the L3 stage using reagents specific for the different phases of the cell cycle. We first performed EdU incorporation experiments to identify cells in S-phase. When EdU was incorporated in the tracheal system for 1 hour (Fig. 3A) at the L3 stage many SB tracheoblasts in Zones 1-3 were found to be in S phase. Interestingly, we found that Btl/Hnt-positive cells in Zone 1 have larger nuclei with twice as much DNA than Cut-positive cells of Zones 2 and 3, as quantified by measuring DAPI fluorescence (Fig. 3C). Zone 1 most likely corresponds to differentiated cells undergoing endoreplication, a modified cell cycle where G1 and S-phases oscillate without cell division. To test whether Zone 1 cells endoreplicate, we examined the expression of the endocycle marker Fizzy-related (Fzr) and the mitotic markers Cyclin B (CycB) and Cyclin A (CycA), as well as phospho-histone H3 (pH3), which labels mitotic cells in the G2/M transition (Shibata et al., 1990). As expected, Fzr is activated in Zone 1 cells but not in cells of Zones 2-4 (Fig. 3E). Fzr expression is maintained during development and Fzr-positive cells continue to grow during pupal stages as shown by DNA content quantification (Fig. 3G,H). By contrast, the mitotic cyclins, CycB (Fig. 3B″) and CycA (not shown), and pH3 (Fig. 3B,B′) were not expressed in Zone 1. We conclude that Zone 1 contains cells undergoing endoreplication and differentiation, and express high levels of Btl and Hnt. Moreover, consistent with their differentiated state, Btl/Hnt-positive cells of Zone 1 collectively migrate towards the posterior of the animal shortly after pupariation. Time-lapse confocal imaging of live pupae expressing GFP driven by *btl-Gal4* revealed that Zone 1 cells extend cytoplasmic extensions and move as a group on the DT (see Fig. S1D in the supplementary material).

Our cell cycle analysis indicates that Cut-positive cells in SB Zones 2 and 3 are mitotically active, as they express CycA, CycB, incorporate EdU and stain positively for pH3 (Fig. 3A,B). Interestingly, pH3 immunoreactivity was detected only in Zones 2 and 3, albeit at different frequencies. Specifically, Zone 2, where

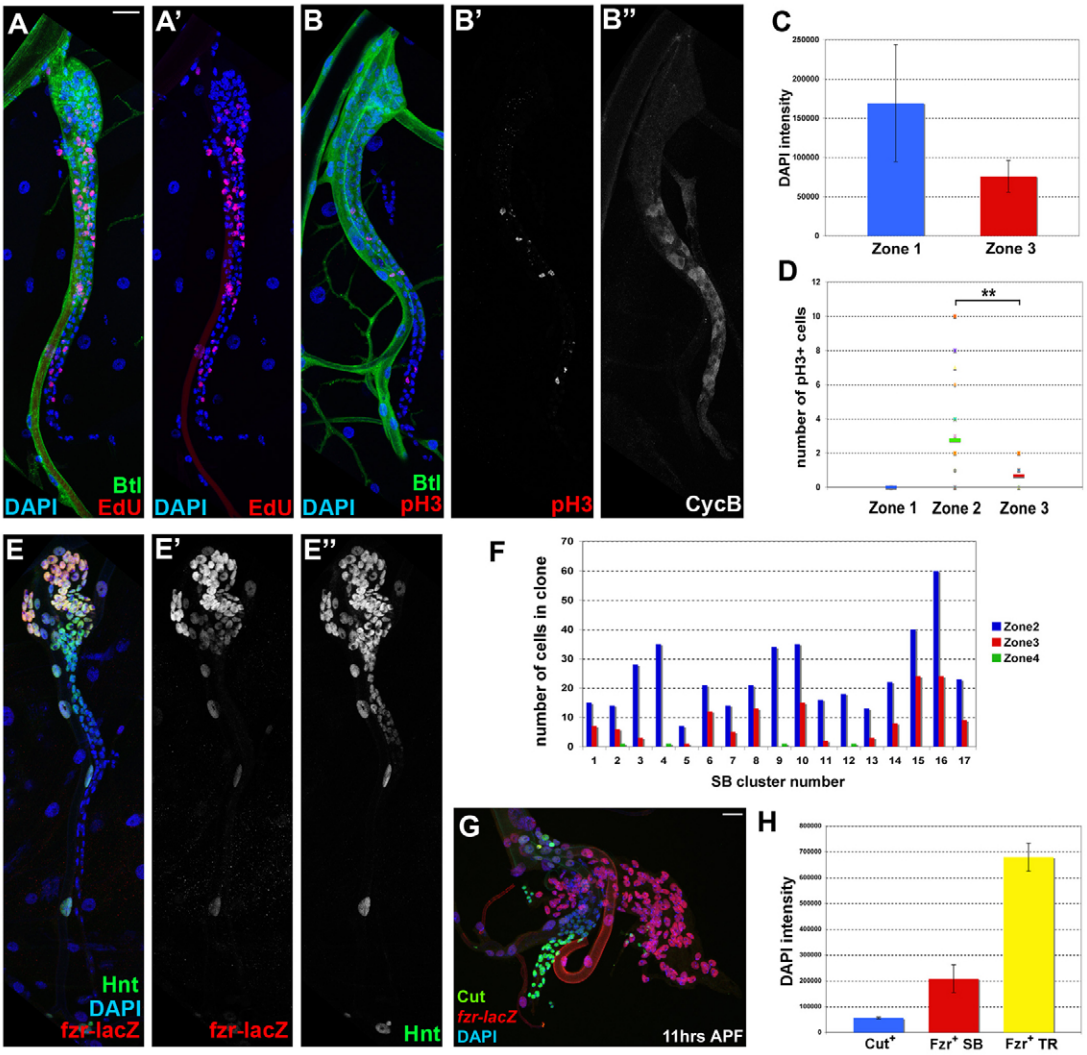

Fig. 3. The SB consists of dividing Cut-positive cells and endocycling Hnt/Btl-positive cells. (**A**,**A′**) SB cells of *btl-Gal4 UAS-GFP* (green) L3 larva undergoing S-phase labeled with EdU (red in A,A′); EdU-positive cells are found throughout the SB. (**B-B″**) SB tracheoblasts of *btl-Gal4 UAS-GFP* (green) L3 larva stained for pH3 (red in B,B′) and Cyclin B (white in B″). DAPI is blue in A,B. (**C**,**C′**) DAPI quantification of Zone 1 and Zone 3 cells; at the late L3 stage, Zone 1 cells have approximately twice as much DNA than do Zone 3 cells (n=40 cells, P<0.001). (**D**) Number of pH3+ cells in different SB Zones. Zones 2 and 3 contain, on average, 2.75 and 0.66 pH3+ cells, respectively (n=24 SBs, P<0.001). (**E-E″**) Fzr-*lacZ* (red in E,E′) coincides with Hnt-positive Zone 1 tracheoblasts (green in E,E″). DAPI is blue in E. (**F**) Graph of heat-shock-induced mitotic clones in the different SB zones. Seventeen SB clusters were analyzed that each contained two or three clones, encompassing cells in Zone 2, Zone 3 and/or Zone 4. Zone 2 clones proliferate faster (larger size) compared with synchronous Zone 3 or 4 clones. Zone 4 clones are induced infrequently and contain one or two cells that do not proliferate during larval stages. (**G**) Tr5 tracheal metamere of a *Fzr-lacZ* 11 hour APF pupa stained for β-galactosidase (red), Cut (green) and DAPI (blue). (**H**) DAPI quantification of the different SB populations from images similar to the one in G. Cut+=Zone 3 cells; Fzr+SB=Zone 1 cells; Fzr+TR=mature tracheal cells. Scale bars: in A, 20 μm for A-E″; in G, 20 μm.

Cut, Hnt, Btl and Esg are expressed at low levels, contains 4.16 times more pH3+ cells than Zone 3, where only Cut expression is observed [average of 2.75 and 0.66 pH3+ cells per SB, respectively (n=24 SBs) (Fig. 3D)]. Altogether, these observations suggest that only Zone 2 and 3 tracheoblasts divide, with Zone 2 cells dividing more frequently, suggesting that Zone 2 constitutes a growth zone.

To test whether Zone 2 cells proliferate faster than those in Zone 3, we induced mitotic clones positively labeled with GFP using the FLPout (Ito et al., 1997) and the MARCM (Lee and Luo, 2001) methods. We induced clones by heat shocking L2 larvae, at a time when SB cells are not yet proliferating, and analyzed the clones during late L3. We scored animals that only contained two or three clones in different SB zones (n=17 SBs) to compare their size. As the clones were induced by heat shock, we expect them to contain the same number of cells if they divide at the same rate in the different SB zones. However, if Zone 2 cells divide faster, as suggested by the increased number of pH3+ cells in this zone, then we expect that clones in Zone 2 would be larger than those in Zone 3. Consistent with Zone 2 cells proliferating faster than those in Zone 3, clones including cells in Zone 2 contained on average 2.4±0.75 times more cells than those in Zone 3 (n=11 SBs) (Fig. 3F). Thus, we conclude that although both Zone 2 and 3 cells are mitotically active, low Cut-expressing Zone 2 cells divide at a faster rate and potentially correspond to a growth zone.

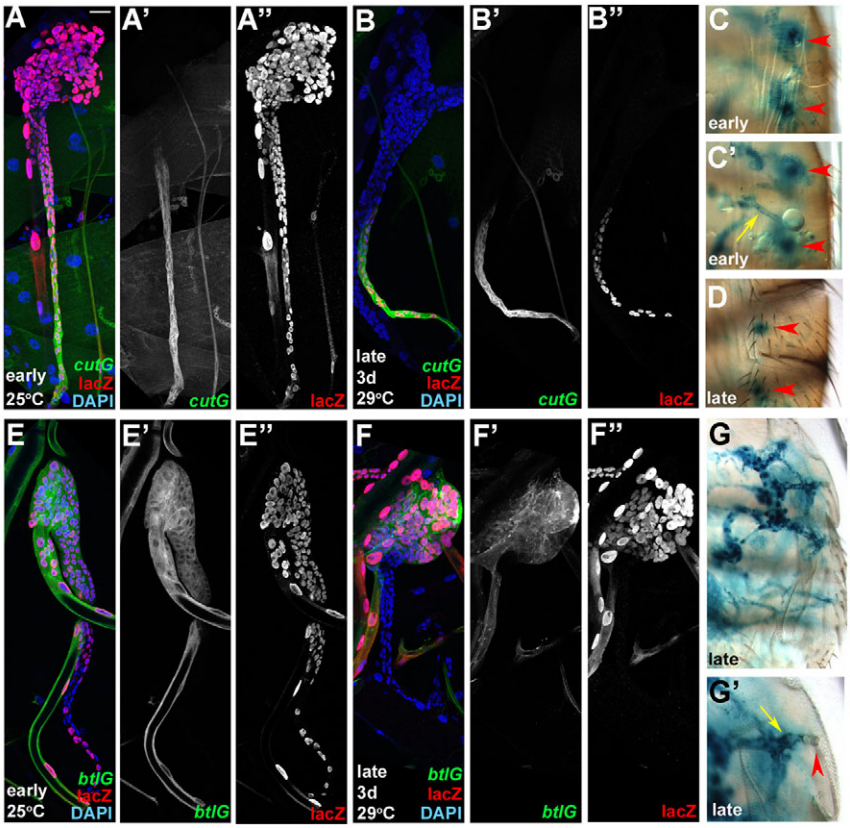

Fig. 4. SB larval tracheoblasts originate from multipotent embryonic Cut-positive cells. (**A-A″**) Early lineage clone of a *UAS-FLP/cut-Gal4; UAS-srcGFP/act5C-FRT-stop-FRT-lacZ* larva reared at 25°C; the Gal4 expression domain is GFP+ (green in A,A′) and the lineage-traced cells are LacZ+ (red in A,A″). All SB cells are LacZ+. (**B-B″**) Late lineage clone of a *UAS-FLP/cut-Gal4 tub-Gal80^{ts}; UAS-srcGFP/ act5C-FRT-stop-FRT-lacZ* larva kept at 18°C and shifted to 29°C 3 days before dissection; only cells in Zone 3 are LacZ+. (**C**,**C′**) X-gal staining of the adult abdomen of a *UAS-FLP/cut-Gal4; UAS-srcGFP/act5C-FRT-stop-FRT-lacZ* animal reared at 25°C, showing LacZ+ cells in the spiracles and tracheal tubes. C and C′ correspond to surface and internal focal planes, respectively. (**D**) X-gal staining of adult abdomen of a *UAS-FLP/cut-Gal4 tub-Gal80^{ts}; UAS-srcGFP/act5C-FRT-stop-FRT-lacZ* lineage-traced animal showing restriction of signal to the spiracles. (**E-E″**) Early lineage clone of a *UAS-FLP; btl-Gal4 UAS-srcGFP/act5C-FRT-stop-FRT-lacZ* larva reared at 25°C; the Gal4 expression domain is GFP+ (green in E,E′) and the lineage-traced cells are LacZ+ (red in E,E″). The presence of LacZ+ cells in Zone 3 indicates that early *btl-Gal4*-expressing cells contribute to Zone 3. (**F-F″**) Late lineage clone of a *UAS-FLP/tub-Gal80^{ts}; btl-Gal4 UAS-srcGFP/act5C-FRT-stop-FRT-lacZ* larva kept at 18°C and shifted to 29°C 3 days before dissection; only cells in Zone 1 are LacZ+, indicating that at this stage the SB cells are restricted. (**G**,**G′**) X-gal staining of adult abdomen of *UAS-FLP/tub-Gal80^{ts}; btl-Gal4 UAS-srcGFP/act5C-FRT-stop-FRT-lacZ* lineage-traced animal showing restriction of the LacZ+ cells to the tracheal tubes. (G′) Twofold magnification of E. In C,D,G′, red arrowheads indicate the spiracles and yellow arrows indicate the tracheal tubes. In A,B,E,F, DAPI is blue. Scale bar: 20 μm in A-B″,E-F″.

Finally, Zone 4 cells did not show any signs of proliferation, nor did they incorporate EdU at the L3 stage, consistent with their arrest in G2 (Ninov et al., 2007; Roseland and Schneiderman, 1979). Furthermore, our mitotic clone analysis shows that when clones are generated in Zone 4, as described above, they contain one or two cells at most, while their synchronous clones in other zones are much larger (Fig. 3F), suggesting that Zone 4 cells are arrested in the cell cycle and do not proliferate during larval stages. Spiracular histoblasts of Zone 4 start proliferating during pupariation along with the rest of the abdominal histoblast nests to generate the adult abdominal epidermis (Ninov et al., 2007), and as they do not contribute to the functional adult airways, they will not be considered further in this study.

In conclusion, our cell cycle analyses reveal that Zone 1 SB tracheoblasts enter the endocycle and start differentiating in late L3; Zones 2 and 3 tracheoblasts proliferate, with Zone 2 cells proliferating at a faster rate; and Zone 4 cells do not proliferate but remain arrested in G2 and begin proliferating during pupal stages.

Cut-expressing cells are the progenitors of all the different cell types of the late L3 SB

Our developmental analysis of SB morphogenesis indicates that SB tracheoblasts arise from few embryonic progenitors that proliferate, differentiate and migrate (Fig. 2). The diversity of the SB cell types at the L3 stage could arise either during development or it could be established at the embryonic stage if cells in different locations are already destined to generate a single cell type/zone. Furthermore, our cell cycle analysis suggests that Zone 2 corresponds to a growth zone. To understand the potency of the SB cells at different developmental stages, we decided to generate a fate map of the various SB cell types. Thus, we performed lineage analysis experiments using the ‘FLP-out’ lineage tracing method (Struhl and Basler, 1993). This method allows permanent β-galactosidase labeling of cells (referred to as LacZ+ cells) that activate the FLPase (see Materials and methods) and, in combination with the Gal4-UAS system (Brand and Perrimon, 1993), permits the tracing of cells that express a Gal4 of interest. To trace the fate of the different zones of SB cells, we expressed FLP with (1) *cut-Gal4*

(Bourbon et al., 2002), which faithfully recapitulates Cut protein expression in the larval tracheal system starting in the embryo (it is expressed in all SB progenitors in the embryo and its expression is maintained in Zones 2 and 3, Fig. 2A,B); and (2) *btl-Gal4* (Ohshiro and Saigo, 1997), the expression of which begins in SB cells during early L3 at the SB/TC junction and is maintained in Zones 1 and 2 (Fig. 2D-J). Thus, expression of *cut-Gal4* and *btl-Gal4* is complementary and the two overlap in Zone 2. Using both drivers, we induced two types of lineage clones: (1) early clones in which FLP expression is initiated at the time of Gal4 activation; and (2) late clones in which FLP expression is regulated by Gal80^{ts} and activated at the early L3 stage.

To assess whether the embryonic Cut-positive SB cells (Fig. 2A) are the progenitors of the L3 SB tracheoblasts, we generated early clones and found that all late L3 SB tracheoblasts in Zones 1-4 are LacZ+ (Fig. 4A). Furthermore, when we followed the fate of these lineage clones in adults, early clones gave rise to the adult external respiratory organs, the spiracles, as well as the gas-transporting tracheal tubes (Fig. 4C). By contrast, when we induced late clones, LacZ+ cells were restricted to Zone 3 (Fig. 4B) and contributed only to the spiracles (Fig. 4D), indicating that at the time of clone induction the different SB zones are already destined to generate different parts of the adult airways. Thus, Cut-positive embryonic SB cells are multipotent, give rise to different cell populations in the L3 larvae and contribute to the entire adult tracheal system, whereas Cut-positive L3 cells have lost their multipotency and only contribute to the spiracle.

When we analyzed the fate of *btl-Gal4*-expressing cells, we found that late clones were only able to label Zone 1 SB cells at the late L3 stage (Fig. 4F) and contributed only to gas-transporting tubes and not to the spiracles in the adult (Fig. 4G). This finding is consistent with the late *cut-Gal4* lineage clones and provides further proof that Zones 1 and 3 are specified at the L3 stage. Interestingly, when we induced early *btl-Gal4* clones (at the initiation of Btl expression in early L3), LacZ+ cells were not restricted to Zones 1 and 2, but were also detected in Zones 3, indicating that *btl-Gal4* cells in the early larvae generate Zone 3 cells in the L3 (Fig. 4E). All 23 SBs with early *btl-Gal4* clones contained LacZ+ cells in Zone 3 and 11 of these contained clones that were spanning the whole length of Zone 3 and extended in Zone 4. This further supports the idea that a growth zone (Zone 2) is established early during development of the SB at the TC/SB junction, a region where we detected more mitotic activity in L3 (Fig. 3B,E). Thus, the position of SB cells at late L3 specifies their fate in the adult, with Zone 1 generating the tracheal tubes and Zone 3 generating the spiracles (Fig. 5). Furthermore, Zone 2 appears to behave as a growth zone at the L3 stage and contributes to cells in both Zones 1 and 3.

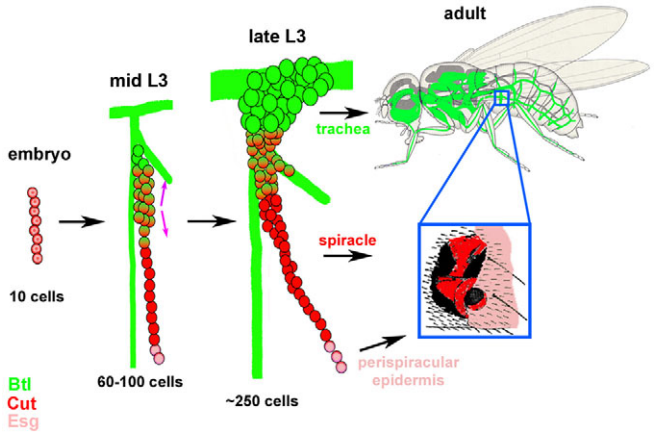

Fig. 5. Model of the development of the SB tracheoblasts. Fate map of the SB tracheoblasts highlighting the destiny of the SB cells in the larval and the adult tracheal system.

Cut is necessary for SB cell survival and suppresses tracheal differentiation

The expression of Cut in the multipotent SB progenitors as well as its dynamic expression in the growing SB indicates that the protein is important for development of the adult *Drosophila* airways. To assess the function of Cut in the developing SB, we performed loss-of-function as well as gain-of-function experiments.

To eliminate Cut from SB tracheoblasts, we used a protein null allele of the gene *cut^{DB7}* (Sun and Deng, 2005) to generate mosaics by conventional mitotic recombination (Xu and Rubin, 1993). This method allows us to compare the size of the mutant clone to that of the wild-type twin spot. We found that *cut^{DB7}* mutant clones contain about half the number of cells of their wild-type twin spots, with an average of 12.7 cells and 23.6 cells, respectively (n=18 clones, Fig. 6D,E). The reduced number of cells in the *cut^{DB7}* mutant clones could reflect either a decrease in cell proliferation or an increase in cell death. To test these possibilities, we stained *cut^{DB7}* clones with CycA, CycB and cleaved caspase 3 antibodies to monitor the state of cell proliferation and cell death, respectively. We found that, whereas CycB (Fig. 6C,C′) and CycA (not shown) accumulation in mutant clones remained largely unchanged, a number of cells showed caspase 3 immunoreactivity (Fig. 6B,B′), whereas in wild-type SBs we rarely detect apoptotic cells (Fig. 6A). Thus, in SB tracheoblasts loss of Cut activity is associated with apoptosis.

To test the role of Cut on the development of the adult abdominal tracheal system, we used a *UAS-cut^{RNAi}* transgene that can effectively suppress Cut protein expression (supplementary material Fig. S2A) to knock down Cut from different SB populations. In agreement with the observed apoptosis in the null clones, when *UAS-cut^{RNAi}* was overexpressed in the SB cells using *esg-Gal4*, which allows expression of the transgene from the embryonic stage, we observed cell death of the larval SB tracheoblasts, breaks in the normal tracheal branches and loss of spiracles as well as necrotic tracheal tissue in the rare adult escapers (supplementary material Fig. S2B-D). Therefore, disruption of Cut expression either by tissue-specific RNAi or by mutant mitotic clones leads to cell death, loss of tissue integrity and loss of spiracles in the adult.

In addition to, and consistent with, the observation that Cut expression is crucial for SB development, ectopic expression of a *UAS-cut* transgene in the *btl-Gal4* domain prevented normal growth of SB tracheoblasts. More specifically, Zone 1 of SB cells ectopically expressing *UAS-cut* under *btl-Gal4* consisted of SB cells with small nuclei (Fig. 6F). As expression of Cut in Zone 1 leads to small cells, it is possible that ectopic Cut might block differentiation and endoreplication in Zone 1 and therefore suppress *Fzr-lacZ* expression. To test this possibility, we induced FLPout clones overexpressing Cut in Zone 1 and found that they contain small cells lacking *Fzr-lacZ* expression (Fig. 6G,H). Therefore, Cut is sufficient to inhibit differentiation/endoreplication of Zone 1 cells.

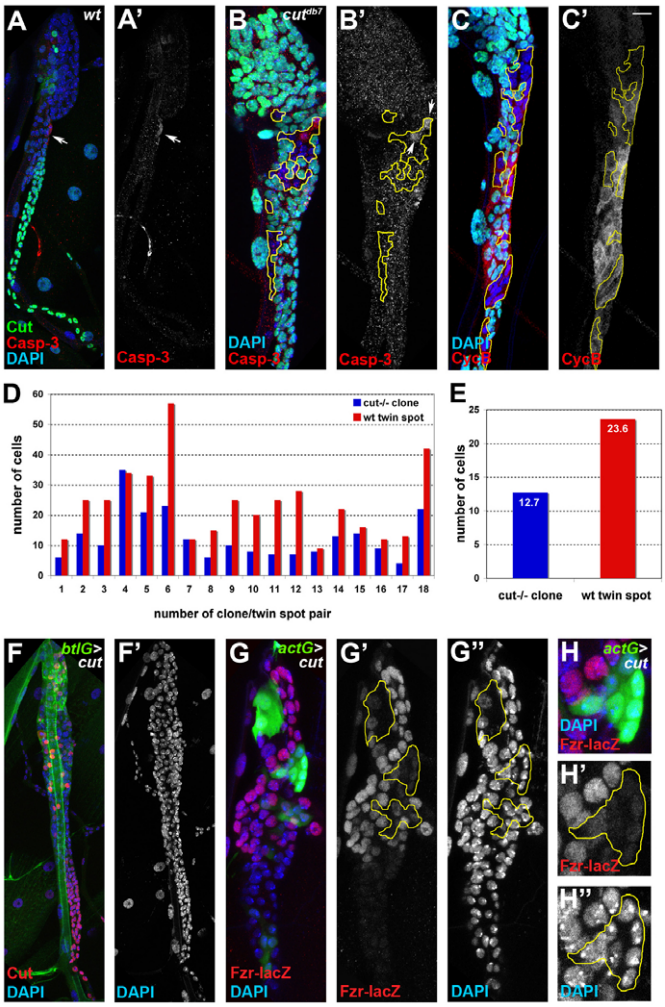

Fig. 6. Cut is necessary for SB tracheoblast survival and morphogenesis of the adult airways. (**A**,**A′**) Wild-type late third instar larva stained for Cut (green), caspase 3 (red) and DAPI (blue). (**B**,**B′**) *cut*^{DB7} mutant clones (lack of GFP) stained with caspase 3 (red) and DAPI (blue). (**C**,**C′**) *cut*^{DB7} mutant clones (lack of GFP) stained with Cyclin B (red) and DAPI (blue). Cells in the upper clone found in Zone 2 have slightly larger nuclei. (**D**) Graph comparing *cut*^{DB7} mutant clones with their wild-type twin spots. Cells of 18 mosaic pairs were analyzed demonstrating that *cut*^{DB7} clones contain about half the number of cells compared with their wild-type twin spots. (**E**) Graph showing the average number of cells in *cut*^{DB7} clones and their wild-type twin spots (from D). (**F**,**F′**) *tub-Gal80*^{ts}*; btl-Gal4 UAS-srcGFP/UAS-cut* larva reared at 25°C stained for Cut (red) and DAPI (blue). (**G-G″**) FLPout clones overexpressing *cut* (green) in Zone 1 suppress *Fzr-lacZ* expression (red in G,G′) and differentiation (small nuclei). DAPI is blue in G,G″. (**H-H″**) Higher magnification view of clone shown in G. Yellow lines delineate the clone in G,H. Scale bar in C′: 20 μm in A,A′,F,F′; 10 μm in B-C′,G-G″; 5 μm in H-H″.

In conclusion, loss- and gain-of-function analyses show that the homeobox transcription factor Cut is crucial for normal SB development and formation of the adult abdominal tracheal system. In particular, Cut is necessary for survival of SB cells during development and subsequent morphogenesis of the adult spiracles and trachea. In addition, ectopic expression of Cut inhibits tracheal cell differentiation by inhibiting Fzr and endoreplication.

DISCUSSION

Larval tracheoblasts and the remodeling of *Drosophila* airways

Adult organs of holometabolous insects such as *Drosophila* are generated by imaginal progenitors that proliferate and differentiate during larval and pupal stages. Imaginal progenitors can either generate an adult organ de novo or they can extensively remodel a pre-existing organ. Organs that are exclusively functional in the adult such as the wings and legs, are generated de novo, whereas others (such as the trachea, the epidermis and the muscle) that are functional throughout life, undergo extensive remodeling during pupariation in a process during which the larval organ is used as a scaffold.

The *Drosophila* adult tracheal system follows the general framework of the embryonic/larval trachea and consists of the tracheal tubes and spiracles. During metamorphosis it remains functional, while at the same time imaginal progenitors extensively remodel the developing adult airways. At this stage, the Tr6-Tr10 tracheal metameres are lost, and although Tr6-Tr9 are restored in the adult, Tr10 is not (Whitten, 1980). In addition, during pupariation, the head and thoracic tracheal system undergoes dramatic remodeling that results in greatly dilated air sacs that oxygenate the brain and the flight muscles, respectively (Sato and Kornberg, 2002; Whitten, 1980). Until recently, it was thought that the fly trachea was remodeled only by imaginal tracheoblasts located on the SB (Manning and Krasnow, 1993; Robertson, 1936; Whitten, 1980). Recent studies, however, have characterized different populations of tracheoblasts at various positions along the larval body (Cabernard and Affolter, 2005; Guha and Kornberg, 2005; Guha et al., 2008; Sato et al., 2008; Sato and Kornberg, 2002; Weaver and Krasnow, 2008) such as: (1) the ASP tracheoblasts located in the adepithelial layer of the wing imaginal disc that generate the thoracic air sacs; and (2) the Tr2 and DB tracheoblasts that remodel part of the tracheal system of the thorax and abdomen, respectively; both correspond to differentiated tracheal tubes that dedifferentiate to reinitiate a proliferation program. Therefore, the adult *Drosophila* tracheal system is generated both by dedicated progenitors and by de-differentiating larval cells that reside in various locations in the larval body.

The SB tracheoblasts and the formation of the abdominal trachea

Our analysis of the morphogenesis of the abdominal SB tracheoblasts demonstrates that the abdominal spiracles, the perispiracular epidermis and the trachea are formed through coordinated proliferation and differentiation of a few multipotent embryonic progenitors (Fig. 5). Although the common origin of spiracles and perispiracular epidermis has previously been shown (Robertson, 1936) using clonal experiments in the abdominal epidermis, studies of gynandromorphs and microcautery, the fact that a common progenitor generates not only these tissues but also the tracheal tubes was not known. More specifically, we show that the Cut/Esg-positive SB embryonic progenitors proliferate and differentiate to generate four zones of SB cells by the late L3 stage. Interestingly, Zone 2 of the SB cluster behaves as a growth zone during early larval stages and produces progeny that contribute to all other zones, which later differentiate into different parts of the functional adult airways (tracheal tubes and spiracles) as well as the epidermis surrounding the spiracles (Fig. 5). This type of morphogenesis is strikingly different from that of the embryonic tracheal system, which does not require cell division, or the development of the posterior spiracles of the larva, which are

generated by the fusion of specialized epidermal structures with the tracheal tubes (Hu and Castelli-Gair, 1999; Samakovlis et al., 1996a).

Here, we present a detailed analysis of the tracheal metameres Tr4 and Tr5, the SB cells of which are responsible for the generation of pupal tracheoles in addition to the adult abdominal airways (Weaver and Krasnow, 2008) (this work). Nevertheless, we also found that the SB tracheoblasts of all posterior tracheal metameres (Tr6-Tr10) express the same markers, i.e. Cut, Esg, Hnt and Btl during larval stages (not shown). These larval cells arise from the embryonic SB clusters and generate the adult trachea and spiracles of the posterior abdomen, although they do not contribute to pupal tracheoles (Manning and Krasnow, 1993; Whitten, 1980). We have found that the Tr6-Tr10 SB cells are fewer in number compared with the Tr4 and Tr5, because they contain fewer cells in Zone 1 (not shown). As Zone 1 cells generate the adult trachea as well as pupal tracheoles, and the latter are generated early during pupariation (Weaver and Krasnow, 2008), we expect that the limited number of Btl cells of Tr6-Tr9 will generate the adult tracheal tubes.

The role of Cut in SB morphogenesis and airway development

In the SB tracheoblasts Cut is expressed throughout the progenitor population at the time of its specification in the embryo, whereas later during development it displays a dynamic graded expression pattern. Interestingly, levels of Cut seem to specify different SB cell populations and growth activities.

Drosophila Cut is a DNA-binding transcription factor with a unique homeodomain and three Cut repeats (Blochlinger et al., 1993; Nepveu, 2001). Expression of Cut at the wing D/V boundary, in postmitotic sensory organs during neurogenesis, cone cells in the eye, Malpighian tubules, posterior larval spiracles and differentiated brain neurons, indicates that *Drosophila* Cut is generally involved in terminal differentiation (Nepveu, 2001). An exception is the follicular epithelium of the *Drosophila* ovary where Cut is necessary for cell proliferation and regulates the mitotic cycle/endocycle switch (Sun and Deng, 2005; Sun and Deng, 2007). Our data on the SB tracheoblasts implicate Cut in cell division as well as cellular differentiation. Interestingly, graded expression of Cut correlates with differential growth activities and differentiation of SB tracheoblasts. Therefore, it seems that Cut is a crucial determinant of cell fates during remodeling of the *Drosophila* trachea.

Importantly, the mammalian Cut homologue Cux1 is expressed in many tissues, including the lung and kidney, its function is often associated with cell cycle control (Sharma et al., 2004) and its expression is elevated in epithelial cancers (Sansregret and Nepveu, 2008). Interestingly, *Cux1* knockout mice die shortly after birth because of delayed differentiation of lung epithelia (Ellis et al., 2001). Furthermore, in the kidney, Cux1 expression during development is inversely related to the degree of cellular differentiation (Vanden Heuvel et al., 2005). Further experiments that will allow precise manipulation of Cut levels will elucidate the molecular mechanism of its action in *Drosophila* and potentially shed light on its function in mammalian tubular organ development.

Concluding remarks

We have focused here on the morphogenesis of the abdominal SB tracheoblasts, the dedicated imaginal progenitors of the adult *Drosophila* tracheal system that remodel the airways, and illustrate how a multipotent population of cells develops through spatially activated proliferation and differentiation to form a functional adult tubular organ. As proliferation and differentiation of airway progenitors are coordinated during SB morphogenesis as well as during mammalian tubular organ development, studies of the remodeling of the tracheal system in *Drosophila* might shed light on mammalian tubular organ development and homeostasis.

Acknowledgements

We thank Yiorgos Apidianakis, Richard Binari, Nikolaos Giagtzoglou, Michele Markstein and Bernard Mathey-Prevot for critical reading of the manuscript, and Carla Kim and members of the Perrimon lab for discussions. We thank the DSHB, Bloomington Stock Center, GETB, VDRC and TRiP for antibodies and fly stocks, and Christos Delidakis, Wu-Min Deng and Gary Struhl for fly stocks. C.P. was supported by an EMBO fellowship (LTF900-2005). N.P. is an Investigator of the HHMI. Deposited in PMC for release after 6 months.

Competing interests statement

The authors declare no competing financial interests.

Supplementary material

Supplementary material for this article is available at
http://dev.biologists.org/lookup/suppl/doi:10.1242/dev.056408/-/DC1

References

Blochlinger, K., Jan, L. Y. and Jan, Y. N. (1993). Postembryonic patterns of expression of *cut*, a locus regulating sensory organ identity in *Drosophila*. *Development* **117**, 441-450.

Bourbon, H. M., Gonzy-Treboul, G., Peronnet, F., Alin, M. F., Ardourel, C., Benassayag, C., Cribbs, D., Deutsch, J., Ferrer, P., Haenlin, M. et al. (2002). A P-insertion screen identifying novel X-linked essential genes in *Drosophila*. *Mech. Dev.* **110**, 71-83.

Brand, A. H. and Perrimon, N. (1993). Targeted gene expression as a means of altering cell fates and generating dominant phenotypes. *Development* **118**, 401-415.

Budnik, V., Gorczyca, M. and Prokop, A. (2006). Selected methods for the anatomical study of *Drosophila* embryonic and larval neuromuscular junctions. *Int. Rev. Neurobiol.* **75**, 323-365.

Cabernard, C. and Affolter, M. (2005). Distinct roles for two receptor tyrosine kinases in epithelial branching morphogenesis in *Drosophila*. *Dev. Cell* **9**, 831-842.

Dietzl, G., Chen, D., Schnorrer, F., Su, K. C., Barinova, Y., Fellner, M., Gasser, B., Kinsey, K., Oppel, S., Scheiblauer, S. et al. (2007). A genome-wide transgenic RNAi library for conditional gene inactivation in *Drosophila*. *Nature* **448**, 151-156.

Duffy, J. B., Harrison, D. A. and Perrimon, N. (1998). Identifying loci required for follicular patterning using directed mosaics. *Development* **125**, 2263-2271.

Ellis, T., Gambardella, L., Horcher, M., Tschanz, S., Capol, J., Bertram, P., Jochum, W., Barrandon, Y. and Busslinger, M. (2001). The transcriptional repressor CDP (Cutl1) is essential for epithelial cell differentiation of the lung and the hair follicle. *Genes Dev.* **15**, 2307-2319.

Fuse, N., Hirose, S. and Hayashi, S. (1994). Diploidy of *Drosophila* imaginal cells is maintained by a transcriptional repressor encoded by *escargot*. *Genes Dev.* **8**, 2270-2281.

Ghabrial, A., Luschnig, S., Metzstein, M. M. and Krasnow, M. A. (2003). Branching morphogenesis of the *Drosophila* tracheal system. *Annu. Rev. Cell Dev. Biol.* **19**, 623-647.

Guha, A. and Kornberg, T. B. (2005). Tracheal branch repopulation precedes induction of the *Drosophila* dorsal air sac primordium. *Dev. Biol.* **287**, 192-200.

Guha, A., Lin, L. and Kornberg, T. B. (2008). Organ renewal and cell divisions by differentiated cells in *Drosophila*. *Proc. Natl. Acad. Sci. USA* **105**, 10832-10836.

Hacohen, N., Kramer, S., Sutherland, D., Hiromi, Y. and Krasnow, M. A. (1998). *sprouty* encodes a novel antagonist of FGF signaling that patterns apical branching of the *Drosophila* airways. *Cell* **92**, 253-263.

Hayashi, S., Hirose, S., Metcalfe, T. and Shirras, A. D. (1993). Control of imaginal cell development by the *escargot* gene of *Drosophila*. *Development* **118**, 105-115.

Hogan, B. L. and Kolodziej, P. A. (2002). Organogenesis: molecular mechanisms of tubulogenesis. *Nat. Rev. Genet.* **3**, 513-523.

Hu, N. and Castelli-Gair, J. (1999). Study of the posterior spiracles of *Drosophila* as a model to understand the genetic and cellular mechanisms controlling morphogenesis. *Dev. Biol.* **214**, 197-210.

Ito, K., Awano, W., Suzuki, K., Hiromi, Y. and Yamamoto, D. (1997). The *Drosophila* mushroom body is a quadruple structure of clonal units each of which contains a virtually identical set of neurones and glial cells. *Development* **124**, 761-771.

LaBarge, M. A., Petersen, O. W. and Bissell, M. J. (2007). Of microenvironments and mammary stem cells. *Stem Cell Rev.* **3**, 137-146.
Lee, T. and Luo, L. (2001). Mosaic analysis with a repressible cell marker (MARCM) for *Drosophila* neural development. *Trends Neurosci.* **24**, 251-254.
Lu, P., Sternlicht, M. D. and Werb, Z. (2006). Comparative mechanisms of branching morphogenesis in diverse systems. *J. Mammary Gland Biol. Neoplasia* **11**, 213-228.
Manning, G. and Krasnow, M. A. (1993). *Development of the Drosophila Tracheal System.* New York: Cold Spring Harbor Laboratory Press..
McGuire, S. E., Mao, Z. and Davis, R. L. (2004). Spatiotemporal gene expression targeting with the TARGET and gene-switch systems in *Drosophila*. *Sci. STKE* **2004**, pl6.
Micchelli, C. A. and Perrimon, N. (2006). Evidence that stem cells reside in the adult *Drosophila* midgut epithelium. *Nature* **439**, 475-479.
Min, H., Danilenko, D. M., Scully, S. A., Bolon, B., Ring, B. D., Tarpley, J. E., DeRose, M. and Simonet, W. S. (1998). Fgf-10 is required for both limb and lung development and exhibits striking functional similarity to *Drosophila branchless*. *Genes Dev.* **12**, 3156-3161.
Nepveu, A. (2001). Role of the multifunctional CDP/Cut/Cux homeodomain transcription factor in regulating differentiation, cell growth and development. *Gene* **270**, 1-15.
Ninov, N., Chiarelli, D. A. and Martin-Blanco, E. (2007). Extrinsic and intrinsic mechanisms directing epithelial cell sheet replacement during *Drosophila* metamorphosis. *Development* **134**, 367-379.
Ohshiro, T. and Saigo, K. (1997). Transcriptional regulation of breathless FGF receptor gene by binding of TRACHEALESS/dARNT heterodimers to three central midline elements in *Drosophila* developing trachea. *Development* **124**, 3975-3986.
Pitsouli, C. and Delidakis, C. (2005). The interplay between DSL proteins and ubiquitin ligases in Notch signaling. *Development* **132**, 4041-4050.
Rawlins, E. L. (2008). Lung epithelial progenitor cells: lessons from development. *Proc. Am. Thorac. Soc.* **5**, 675-681.
Rawlins, E. L. and Hogan, B. L. (2006). Epithelial stem cells of the lung: privileged few or opportunities for many? *Development* **133**, 2455-2465.
Robertson, C. W. (1936). The metamorphosis of *Drosophila melanogaster*, including an accurately timed account of the principal morphological changes. *J. Morph.* **59**, 351-399.
Roseland, C. and Schneiderman, H. (1979). Regulation of metamorphosis of the abdominal histoblasts of *Drosophila melanogaster*. *Roux's Arch. Dev. Biol.* **186**, 235-265.
Samakovlis, C., Hacohen, N., Manning, G., Sutherland, D. C., Guillemin, K. and Krasnow, M. A. (1996a). Development of the *Drosophila* tracheal system occurs by a series of morphologically distinct but genetically coupled branching events. *Development* **122**, 1395-1407.
Samakovlis, C., Manning, G., Steneberg, P., Hacohen, N., Cantera, R. and Krasnow, M. A. (1996b). Genetic control of epithelial tube fusion during *Drosophila* tracheal development. *Development* **122**, 3531-3536.
Sansregret, L. and Nepveu, A. (2008). The multiple roles of CUX1: insights from mouse models and cell-based assays. *Gene* **412**, 84-94.
Sato, M. and Kornberg, T. B. (2002). FGF is an essential mitogen and chemoattractant for the air sacs of the *Drosophila* tracheal system. *Dev. Cell* **3**, 195-207.
Sato, M., Kitada, Y. and Tabata, T. (2008). Larval cells become imaginal cells under the control of homothorax prior to metamorphosis in the *Drosophila* tracheal system. *Dev. Biol.* **318**, 247-257.
Sharma, M., Fopma, A., Brantley, J. G. and Vanden Heuvel, G. B. (2004). Coexpression of Cux-1 and Notch signaling pathway components during kidney development. *Dev. Dyn.* **231**, 828-838.
Shibata, K., Inagati, M. and Ajiro, K. (1990). Mitosis-specific histone H3 phosphorylation in vitro in nucleosome structures. *Eur. J. Biochem.* **192**, 87-93.
Struhl, G. and Basler, K. (1993). Organizing activity of Wingless protein in *Drosophila*. *Cell* **72**, 527-540.
Sun, J. and Deng, W. M. (2005). Notch-dependent downregulation of the homeodomain gene cut is required for the mitotic cycle/endocycle switch and cell differentiation in *Drosophila* follicle cells. *Development* **132**, 4299-4308.
Sun, J. and Deng, W. M. (2007). Hindsight mediates the role of Notch in suppressing Hedgehog signaling and cell proliferation. *Dev. Cell* **12**, 431-442.
Sutherland, D., Samakovlis, C. and Krasnow, M. A. (1996). *branchless* encodes a *Drosophila* FGF homolog that controls tracheal cell migration and the pattern of branching. *Cell* **87**, 1091-1101.
Tefft, J. D., Lee, M., Smith, S., Leinwand, M., Zhao, J., Bringas, P., Jr, Crowe, D. L. and Warburton, D. (1999). Conserved function of mSpry-2, a murine homolog of *Drosophila sprouty*, which negatively modulates respiratory organogenesis. *Curr. Biol.* **9**, 219-222.
Vanden Heuvel, G. B., Brantley, J. G., Alcalay, N. I., Sharma, M., Kemeny, G., Warolin, J., Ledford, A. W. and Pinson, D. M. (2005). Hepatomegaly in transgenic mice expressing the homeobox gene Cux-1. *Mol. Carcinog.* **43**, 18-30.
Warburton, D., Tefft, D., Mailleux, A., Bellusci, S., Thiery, J. P., Zhao, J., Buckley, S., Shi, W. and Driscoll, B. (2001). Do lung remodeling, repair, and regeneration recapitulate respiratory ontogeny? *Am. J. Respir. Crit. Care Med.* **164**, S59-S62.
Weaver, M. and Krasnow, M. A. (2008). Dual origin of tissue-specific progenitor cells in *Drosophila* tracheal remodeling. *Science* **321**, 1496-1499.
Whitten, J. (1980). *The Post-Embryonic Development of the Tracheal System in Drosophila melanogaster* (ed. T. Wright). New York: Academic Press.
Wilk, R., Reed, B. H., Tepass, U. and Lipshitz, H. D. (2000). The *hindsight* gene is required for epithelial maintenance and differentiation of the tracheal system in *Drosophila*. *Dev. Biol.* **219**, 183-196.
Xu, T. and Rubin, G. M. (1993). Analysis of genetic mosaics in developing and adult *Drosophila* tissues. *Development* **117**, 1223-1237.
Zhou, S., Degan, S., Potts, E. N., Foster, W. M. and Sunday, M. E. (2009). NPAS3 is a *trachealess* homolog critical for lung development and homeostasis. *Proc. Natl. Acad. Sci. USA* **106**, 11691-11696.